Acta Crystallographica Section F
Structural Biology and Crystallization Communications
ISSN 1744-3091

Crystallization, data collection and data processing of maltose-binding protein (MalE) from the phytopathogen *Xanthomonas axonopodis* pv. *citri*

C. S. Souza,[a] L. C. S. Ferreira,[a] L. Thomas,[b] J. A. R. G. Barbosa[c]* and A. Balan[c]*

[a]Departamento de Microbiologia, Instituto de Ciências Biomédicas II, Universidade de São Paulo, São Paulo, SP, Brazil, [b]Howard Hughes Medical Institute, Division of Biology, California Institute of Technology, 1200 East California Boulevard, Pasadena, California, USA, and [c]Center for Structural Molecular Biology (CeBiMe), Brazilian Synchrotron Light Laboratory (LNLS), CP 6192, Campinas, SP 13084-971, Brazil

Correspondence e-mail: joao@lnls.br, abalan@usp.br

Received 27 October 2008
Accepted 9 December 2008

Maltose-binding protein is the periplasmic component of the ABC transporter responsible for the uptake of maltose/maltodextrins. The *Xanthomonas axonopodis* pv. *citri* maltose-binding protein MalE has been crystallized at 293 K using the hanging-drop vapour-diffusion method. The crystal belonged to the primitive hexagonal space group $P6_122$, with unit-cell parameters a = 123.59, b = 123.59, c = 304.20 Å, and contained two molecules in the asymetric unit. It diffracted to 2.24 Å resolution.

1. Introduction

Maltose- or maltodextrin-binding proteins (MBPs) are located in the periplasm of Gram-negative bacterial species, where they interact with substrates such as the disaccharide maltose, longer linear maltodextrins and even larger and more complex cyclodextrin molecules before uptake to the interior of the cell (Boos & Shuman, 1998; Tam & Saier, 1993). In *Escherichia coli* K12, the active transport of maltose and maltodextrins requires MBP and an ATP-dependent membrane-associated transport system made up of two integral membrane proteins (MalF and MalG) and two copies of an ATP-hydrolyzing subunit (MalK) (Hall, Ganesan *et al.*, 1997; Hall, Gehring *et al.*, 1997; Hall, Thorgeirsson *et al.*, 1997). Similar to other ABC-type transport binding components, MBP or MalE typically consists of two nearly symmetrical lobes separated by a hinge region in which the substrate-binding site lies (Spurlino *et al.*, 1991). After binding, the protein undergoes a conformational change as a direct result of bending and twisting movements of the lobes towards each other, leading to substrate enclosure (Quiocho *et al.*, 1997; Saul *et al.*, 2003; Millet *et al.*, 2003; Telmer & Shilton, 2003). MBPs have also been characterized as chemoreceptors for maltose taxis after interaction of the bound complex with the periplasmic portion of the Tar protein (Zhang *et al.*, 1999).

Much of the existing knowledge about microbial ABC transporters has been gleaned from studies of the high-affinity maltose-transport system in *E. coli*. Indeed, *E. coli* MBP (*Eco*_MBP) has been subjected to a battery of genetic, biochemical and biophysical studies that have produced a wealth of information about the structure and ligand-binding properties of *Eco*_MBP (Martineau *et al.*, 1990; Spurlino *et al.*, 1991; Sharff *et al.*, 1992). However, it is unclear to what degree these observations can be generalized to other bacteria: that is, what are the structural similarities and differences between *Eco*_MBP and MBPs from distant relatives such as bacteria living in different habitats or host organisms? The crystal structures of six bacterial MBPs have been reported from *Pyrococcus furiosus* (PDB code 1elj; Evdokimov *et al.*, 2001), *Thermococcus litoralis* (1eu8; Diez *et al.*, 2001), *Alicyclobacillus acidocaldarius* (1urg; Schafer *et al.*, 2004), *E. coli* (1anf; Spurlino *et al.*, 1991), *Thermus thermophilus* (2gh9; M. J. Cuneo, A. Changela, L. S. Beese & H. W. Hellinga, unpublished work) and *Thermotoga maritima* (2fnc; M. J. Cuneo & A. Changela, unpublished work) and they all share a similar structural organization irrespective of the relatively low amino-acid sequence conservation.

The crystal structures of MBPs in the closed and open states reveal a cleft between two lobes in which the oligosaccharide substrate binds

Table 1
Crystallization conditions and resolution obtained for the *Xac*_MalE crystals.

Nd, no diffraction.

Crystallization condition	Additive	Cryoprotectant	Ligand	Resolution (Å)
4% PEG 8000	—	20% glycerol	Maltose	Nd
25% PEG MME 2000	—	15% glycerol	Maltose	Nd
0.1 *M* Na MES pH 6.5, 0.6 *M* sodium chloride, 20% PEG 4000	—	20% glycerol	Maltose	Nd
0.1 *M* Na MES pH 6.5, 12% PEG 20 000	—	—	Maltose	10.0
0.1 *M* Na HEPES pH 7.5, 12% PEG 20 000	—	—	Maltose	7.0
0.1 *M* Na HEPES pH 7.5, 0.2 *M* sodium acetate, 20% PEG 3000	30% dioxane	15% glycerol	Maltose	3.7
0.1 *M* Na HEPES pH 7.5, 0.2 *M* sodium acetate, 20% PEG 3000	—	—	Maltose	3.4
0.1 *M* Na HEPES pH 7.5, 0.2 *M* sodium acetate, 20% PEG 3000	0.1 *M* trimethylamine–HCl	—	Maltose	3.4
0.1 *M* Tris–HCl pH 8.5, 0.2 *M* lithium sulfate, 17% PEG 4000	—	20% glycerol	Maltose	3.2
1.2 *M* sodium tartrate, 0.1 *M* bis-Tris propane pH 7.0	—	25% glycerol	Maltose	2.8
3.5 *M* sodium formate, 0.1 *M* Tris–HCl pH 8.0	—	—	Maltose	2.24

and is completely engulfed by rotation of the lobes. While delivering the substrate to the transmembrane subunits, the binding protein seems to stimulate ATP hydrolysis. The observation that MBP is trapped in a complex with $MalFGK_2$ in the presence of a transition-state analogue (Mg, ADP, vanadate) suggests that the binding of MBP induces conformational changes in the transporter and thereby triggers ATP hydrolysis (Oldham *et al.*, 2007).

However, maltose/maltodextrin-binding proteins from plant-associated bacteria have not been functionally or structurally characterized. The genus *Xanthomonas* comprises a diverse and economically important group of bacterial phytopathogens that belong to the γ-subdivision of the proteobacteria. *Xanthomonas axonopodis* pv. *citri* is the causative agent of citrus canker, a disease that affects several citrus cultivars around the world and that results in significant economic losses worldwide (Brunings & Gabriel, 2003). Definition of the complete genome sequence of *X. axonopodis* pv. *citri* revealed that approximately 4% of the genomic content encoding structural genes is dedicated to the synthesis of ATP-dependent transport systems, represented mainly by ABC transporters (da Silva *et al.*, 2002). Most of the maltose-uptake system is present in a single operon encompassing three cistrons (*malElacFG*) that encode the periplasmic binding protein MalE and two transmembrane proteins LacF and LacG. The nucleotide-binding domain corresponding to the MalK protein was identified in another region of the genome (the *ugpC* gene, which shares 50% sequence identity to *E. coli malK*). The periplasmic protein contains 456 amino acids, including a putative 19-amino-acid signal peptide, and should drive both the specificity and affinity of the maltose/maltodextrin-transport system in this plant pathogen. Previous evidence has suggested that recombinant *X. axonopodis* pv. *citri* MalE (*Xac*_MalE) binds maltose (Balan *et al.*, 2005), but the functionality of this operon in *X. axonopodis* pv. *citri* is still unclear. In order to determinate the three-dimensional structure of this protein in the presence of maltose, we report the crystallization, data collection and initial structural analysis of recombinant *Xac*_MalE expressed in *E. coli*. The X-ray crystal structure of the present protein is expected to reveal structural features that may be common to MBPs from other phytopathogenic microorganisms, since the amino-acid sequences of MalE and of the other components of the transporter share more than 80% identity.

2. Crystallization

The nucleotide sequence encoding mature MalE (without the initial 19-amino-acid signal peptide) was amplified by PCR from *X. axonopodis* pv. *citri* var. 306 and cloned into a pET28a vector (Novagen) for production of a cytoplasmic protein with a His_6 tag genetically fused at the N-terminal end. The recombinant protein was purified from soluble extracts by immobilized nickel-affinity chromatography (1 ml HisTrap HP from Amersham Biosciences; Balan *et al.*, 2005). Samples dialyzed against 20 m*M* Tris–HCl pH 8.0, 50 m*M* NaCl were kept at 277 K at a final concentration of 40 mg ml^{-1}. Samples of recombinant *Xac*_MalE protein (10 mg ml^{-1}) in the absence and the presence of various sugars including maltose, trehalose, lactose, α-cyclodextrin and β-cyclodextrin (the protein:sugar ratio was 1:2) were submitted to crystallization trials using both the sitting-drop and hanging-drop vapour-diffusion methods. Screenings were performed using Crystal Screens 1 and 2, Index Screen, SaltRX and PEG/Ion Screen (all from Hampton Research), JBScreen 1–5 (Jena Bioscience) and Wizard I and II (Emerald Biostructure) according to the instructions of the manufacturers. Drops were prepared by mixing equal volumes (2 µl) of protein and reservoir solution and were equilibrated against 400 µl reservoir solution at 294 K. Refinement of the crystallization conditions was carried out by varying the precipitant and salt concentrations as well as the pH and by the incorporation of additives.

3. Data collection and processing

The final crystallographic data were collected on protein crystallography beamline 9-2 of the Stanford Synchrotron Radiation Laboratory (Menlo Park, California, USA), a national user facility operated by Stanford University on behalf of the US Department of Energy, Office of Basic Energy Sciences and Biological and Environmental Research. The wavelength was 0.82 Å and a MarMosaic

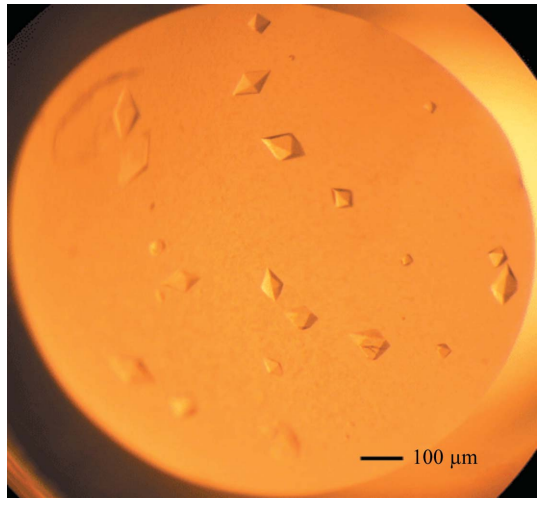

Figure 1
X. axonopodis pv. *citri* MalE crystals obtained in 3.5 *M* sodium formate and 0.1 *M* Tris pH 8.0; the crystals diffracted to 2.24 Å resolution.

Table 2
Data-collection and processing statistics of *X. axonopodis* pv. *citri* MalE crystal.

Values in parentheses are for the last resolution shell.

Space group	$P6_122$
Unit-cell parameters (Å, °)	a = 123.59, b = 123.59, c = 304.20, α = 90.00, β = 90.00, γ = 120.00
Mosaicity (°)	0.24
Temperature (K)	100
Wavelength (Å)	0.84
Oscillation (°)	0.25
Crystal-to-detector distance (mm)	325.0
No. of frames	360
Resolution limits (Å)	50.00–2.24 (2.36–2.24)
$I/\sigma(I)$ after merging	23.1 (4.5)
Completeness (%)	99.9 (99.8)
Multiplicity	10.9 (11.1)
R_{merge}	0.07 (0.45)
No. of reflections	726568 (105326)
No. of unique reflections	66688 (9508)

325 CCD detector was used to record the oscillation data with $\Delta\varphi = 0.25°$. Crystals were cooled in a stream of nitrogen gas at 100 K in order to minimize radiation damage. The data sets were integrated using *MOSFLM* v.6.2.6 (Leslie, 1999) and scaled with *SCALA* v.3.2.19 (Evans, 1993). The Matthews coefficient was calculated using the *CCP*4 package (Collaborative Computational Project, Number 4, 1994).

4. Results and discussion

The single-step purification by affinity chromatography was sufficient to produce crystallization-quality protein (Balan *et al.*, 2005). Crystal growth usually occurred in 6 d, leading to bipyramidal crystals with dimensions ranging from 100 to 500 µm. Crystals were obtained in more than 15 different crystallization conditions containing polyethylene glycol (PEG), MES or HEPES in the pH range 6.5–7.5, but were only obtained in the presence of maltose. However, none of these crystals were capable of generating diffraction patterns with resolution better than 7 Å. Cryoprotection with 15–20% glycerol or PEG 400 and annealing (1–15 s) were tested in order to increase the resolution, with no success. Refinement of all crystallization conditions revealed that crystals grown in 0.1 *M* HEPES pH 7.5 or 0.1 *M* Tris pH 8.0 with lithium sulfate, sodium acetate or sodium formate showed an increase in the resolution limit to around 3.2–3.4 Å (Table 1). All crystallization trials with sugars other than maltose were unsuccessful.

In order to further improve the quality of the crystals, the salt concentration in the samples was increased from 20 to 50 m*M* Tris–HCl and the pH was increased to 8.0. Finally, good diffraction data were obtained to a maximum resolution of 2.24 Å on increasing the pH from 7.0 to 8.0 in 0.1 *M* Tris–HCl and 3.5 *M* sodium formate (Fig. 1). Crystals showed the symmetry and systematic absences of the primitive hexagonal space group $P6_122$. The data-collection statistics are summarized in Table 2. The Matthews coefficient (Matthews, 1968) was calculated to be 3.35 Å^3 Da^{-1} and the solvent content was 63.4% assuming the presence of two molecules in the asymmetric unit.

Ongoing experiments will elucidate the structural organization of *Xac*_MalE, which will shed light on the mechanism of sugar transport in *Xanthomonas* species as well as in other phytopathogenic bacteria. Elucidation of the crystal structure of *Xac*_MalE will also reveal possible conserved structural and functional features that are shared with other substrate-binding proteins of maltose ABC transporters reported from other bacterial and archaeal species.

This work was supported by Fundação de Amparo à Pesquisa do Estado de São Paulo (grants 01/07540-3, 04/02716-4 and 00/10266-8), Conselho Nacional de Desenvolvimento Científico e Tecnológico (CNPq), Associação Brasileira de Tecnologia de Luz Síncrotron (ABTLuS) and the US Department of Energy. We would like to thank Andréia N. Meza and Camila Calderon for their technical assistance and Dr Pamela Bjorkman for allowing part of this research to be carried out in her laboratory.

References

Balan, A., de Souza, C. S., Moutran, A., Ferreira, R. C., Franco, C. S., Ramos, C. H. & Ferreira, L. C. S. (2005). *Protein Expr. Purif.* **43**, 103–110.
Boos, W. & Shuman, H. (1998). *Microbiol. Mol. Biol. Rev.* **62**, 204–229.
Brunings, A. M. & Gabriel, D. W. (2003). *Mol. Plant Pathol.* **4**, 141–157.
Collaborative Computational Project, Number 4 (1994). *Acta Cryst.* D**50**, 760–763.
da Silva, A. C. *et al.* (2002). *Nature (London)*, **417**, 459–463.
Diez, J., Diederichs, K., Greller, G., Horlacher, R., Boos, W. & Welte, W. (2001). *J. Mol. Biol.* **305**, 905–915.
Evans, P. R. (1993). *Proceedings of the CCP4 Study Weekend. Data Collection and Processing*, edited by L. Sawyer, N. Isaacs & S. Bailey, pp. 114–122. Warrington: Daresbury Laboratory.
Evdokimov, A. G., Anderson, D. E., Routzahn, K. M. & Waugh, D. S. (2001). *J. Mol. Biol.* **305**, 891–904.
Hall, J. A., Ganesan, A. K., Chen, J. & Nikaido, H. (1997). *J. Biol. Chem.* **272**, 17615–17622.
Hall, J. A., Gehring, K. & Nikaido, H. (1997). *J. Biol. Chem.* **272**, 17605–17609.
Hall, J. A., Thorgeirsson, T. E., Liu, J., Shin, Y. K. & Nikaido, H. (1997). *J. Biol. Chem.* **272**, 17610–17614.
Leslie, A. G. W. (1999). *Acta Cryst.* D**55**, 1696–1702.
Martineau, P., Saurin, W., Hofnung, M., Spurlino, J. C. & Quiocho, F. A. (1990). *Biochimie*, **72**, 397–402.
Matthews, B. W. (1968). *J. Mol. Biol.* **33**, 491–497.
Millet, O., Hudson, R. P. & Kay, L. E. (2003). *Proc. Natl Acad. Sci. USA*, **100**, 12700–12705.
Oldham, M. L., Khare, D., Quiocho, F. A., Davidson, A. L. & Chen, J. (2007). *Nature (London)*, **450**, 515–521.
Quiocho, F. A., Spurlino, J. C. & Rodseth, L. E. (1997). *Structure*, **5**, 997–1015.
Saul, F. A., Mourez, M., Vulliez-Le, N. B., Sassoon, N., Bentley, G. A. & Betton, J. M. (2003). *Protein Sci.* **12**, 577–585.
Schafer, K., Magnusson, U., Scheffel, F., Schiefner, A., Sandgren, M. O., Diederichs, K., Welte, W., Hülsmann, A., Schneider, E. & Mowbray, S. L. (2004). *J. Mol. Biol.* **335**, 261–274.
Sharff, A. J., Rodseth, L. E., Spurlino, J. C. & Quiocho, F. A. (1992). *Biochemistry*, **31**, 10657–10663.
Spurlino, J. C., Lu, G. Y. & Quiocho, F. A. (1991). *J. Biol. Chem.* **266**, 5202–5219.
Tam, R. & Saier, M. H. Jr (1993). *Microbiol. Rev.* **57**, 320–346.
Telmer, P. G. & Shilton, B. H. (2003). *J. Biol. Chem.* **278**, 34555–34567.
Zhang, Y., Gardina, P. J., Kuebler, A. S., Kang, H. S., Christopher, J. A. & Manson, M. D. (1999). *Proc. Natl Acad. Sci. USA*, **96**, 939–944.